ORIGINAL ARTICLE

Cancer Science WILEY

Tumor suppressive role of the epigenetic master regulator BRD3 in colorectal cancer

Masahiro Hashimoto[1,2] | Takaaki Masuda[1] | Yusuke Nakano[1,2] | Taro Tobo[3] | Hideyuki Saito[1] | Kensuke Koike[1] | Junichi Takahashi[1] | Tadashi Abe[1] | Yuki Ando[1] | Yuki Ozato[1,2] | Kiyotaka Hosoda[1] | Satoshi Higuchi[1,2] | Yuichi Hisamatsu[1] | Takeo Toshima[1] | Yusuke Yonemura[1] | Tsuyoshi Hata[2] | Mamoru Uemura[2] | Hidetoshi Eguchi[2] | Yuichiro Doki[2] | Masaki Mori[4] | Koshi Mimori[1]

[1]Department of Surgery, Kyushu University Beppu Hospital, Beppu, Japan

[2]Department of Gastroenterological Surgery, Osaka University Graduate School of Medicine, Suita, Japan

[3]Department of Pathology, Kyushu University Beppu Hospital, Beppu, Japan

[4]Tokai University School of Medicine, Isehara, Japan

Correspondence
Koshi Mimori, Department of Surgery, Kyushu University Beppu Hospital, Beppu, 874-0838, Japan.
Email: mimori.koshi.791@m.kyushu-u.ac.jp

Abstract

Bromodomain and extraterminal domain (BET) family proteins are epigenetic master regulators of gene expression via recognition of acetylated histones and recruitment of transcription factors and co-activators to chromatin. Hence, BET family proteins have emerged as promising therapeutic targets in cancer. In this study, we examined the functional role of bromodomain containing 3 (BRD3), a BET family protein, in colorectal cancer (CRC). In vitro and vivo analyses using *BRD3*-knockdown or BRD3-overexpressing CRC cells showed that BRD3 suppressed tumor growth and cell cycle G1/S transition and induced p21 expression. Clinical analysis of CRC datasets from our hospital or The Cancer Genome Atlas revealed that BET family genes, including *BRD3*, were overexpressed in tumor tissues. In immunohistochemical analyses, BRD3 was observed mainly in the nucleus of CRC cells. According to single-cell RNA sequencing in untreated CRC tissues, *BRD3* was highly expressed in malignant epithelial cells, and cell cycle checkpoint-related pathways were enriched in the epithelial cells with high *BRD3* expression. Spatial transcriptomic and single-cell RNA sequencing analyses of CRC tissues showed that *BRD3* expression was positively associated with high *p21* expression. Furthermore, overexpression of BRD3 combined with knockdown of, a driver gene in the BRD family, showed strong inhibition of CRC cells in vitro. In conclusion, we demonstrated a novel tumor suppressive role of BRD3 that inhibits tumor growth by cell cycle inhibition in part via induction of p21 expression. BRD3 activation might be a novel therapeutic approach for CRC.

KEYWORDS
bromodomain and extraterminal domain (BET), bromodomain containing 3 (BRD3), cell cycle, cell growth, colorectal cancer

1 | INTRODUCTION

Epigenetic regulation of gene expression is important for controlling cellular functions.[1] Epigenetic regulators alter non-covalent interactions within and between nucleosomes by altering histones and DNA modifications such as DNA methylation, histone acetylation, and histone methylation, leading to altered chromatin structures, followed by target gene expression.[1,2] Epigenetic dysregulation plays a crucial role in cancer progression.[5] For example, epigenetic dysregulation followed by aberrant transcription of driver genes, including the representative oncogenes MYC, CCND1, and CCNA1, has been observed in various malignancies.[3-5] Thus, targeting epigenetic regulation during cancer progression is emerging as a novel therapeutic approach to cancer treatment.

Bromodomain and extraterminal domain (BET) family proteins are epigenetic master regulators that consist of four members (bromodomain containing 2 (BRD2), bromodomain containing 3 (BRD3), bromodomain containing 4 (BRD4), and bromodomain testis associated (BRDT)).[6] Each BET protein promotes gene transcription initiation and elongation by recruiting transcriptional complexes and inducing chromatin remodeling via interactions between their two tandem 110-amino-acid bromodomains (BDs) and the acetylated lysine residues of histones present on the chromatin of target genes.[7] Evidence suggests that BET family proteins may be required for rapid target gene induction.[8]

Of note, BET family proteins are upregulated in various solid tumors, including colorectal cancer (CRC), [9-11] one of the most common types of cancers worldwide. The oncogenic roles of BET family proteins were first revealed in nuclear protein in testis carcinoma and identified as potential therapeutic cancer targets.[12] BRD4, a well studied BET family member, is enriched in numerous enhancer regions and some large super-enhancer regions.[3,6] Overexpression of BRD4 contributes to cancer cell growth and metastasis and is correlated with poor outcomes by promoting the transcription of oncogenes, including MYC and E2F.[11,13-15] BRD2 is reportedly involved in cell cycle regulation and R-point regulation; it forms a complex with transcription factor ELK4 and activates transcription of LAMB3 in CRC, leading to tumor growth and metastasis.[16,17] Hence, BET inhibitors, such as the pan-BET inhibitor JQ1, have emerged as a potential new treatment strategy for gastrointestinal cancers, including CRC.[1,14] Interestingly, it has been reported that the BRD3 expression level may reflect therapeutic efficacy via pan-BET inhibition.[18] Also, in CRC cells, the antiproliferative effects of pan-BET inhibition depend on the cell line.[19] Thus, BRD3 may be involved in therapeutic resistance to BET inhibitors. However, the clinical and biological roles of BRD3 expression remain unclear in cancer cells.

In this study, we revealed a tumor suppressive role of BRD3 in CRC by combining in vitro and in vivo analyses using BRD3-overexpressing or BRD3-knockdown CRC cells with single-cell RNA sequencing (scRNA-seq) and spatial transcriptomic expression analyses using CRC tissues.

2 | MATERIALS AND METHODS

2.1 | CRC patients and clinical sample collection

Primary CRC samples were obtained from 144 patients who had undergone surgery at Kyusyu University Beppu Hospital and affiliated hospitals from 1993 to 2002 (our CRC cohort). All patients had a histological diagnosis of CRC and were treated following the Japanese Society of Cancer of the Colon and Rectum Guidelines for the Treatment of Colorectal Cancer.[20] The study was approved by the Kyushu University Institutional Review Board (approval #22185-00), and informed consent was obtained in the form of an opt-out on the website (https://www.beppu.kyushu-u.ac.jp/geka/). Resected tumor tissues, paired normal tissues, and formalin-fixed paraffin-embedded sections from CRC patients were obtained as described previously.[21]

2.2 | Public datasets

CRC RNA sequencing data from The Cancer Genome Atlas (TCGA) were downloaded from UCSC Xena (http://xena.ucsc.edu/). We obtained gene-level transcription estimates as $\log2(x+1)$ transformed RSEM normalized counts. We also obtained gene expression data by array from CRC organoids from 31 CRC patients from the GSE74843 dataset through the GEO database (https://www.ncbi.nlm.nih.gov/). The data were normalized using the robust multi-array analysis implemented in the R package *affy*, and the mean values of each gene were compared. We attained scRNA-seq data from GSE161277 and spatial transcriptomic data from a spatial transcriptomic website (http://www.cancerdiversity.asia/scCRLM/). The spatial transcriptomic data of one patient (ST-P1) who did not receive neoadjuvant chemotherapy treatment were used. We obtained the normalized read density of ChIP-seq datasets in MM1S cells, a human multiple myeloma cell line. The Integrative Genomics Viewer (IGV) software v2.12.3 was used for a graphic illustration of the ChIP-seq peaks.

2.3 | scRNA-seq data processing

We downloaded 3′end scRNA-seq raw count matrix data (10x Genomics) based on 54,782 cells from three CRC patients from GSE161277. The Python package *Scanpy* (v1.9.3) was used for processing. Briefly, genes detected three cells of the total cells and cells with fewer than 200 expressed genes were removed and selected according to the following criteria: <25% mitochondrial gene expression in unique molecular identifier (UMI) counts. The count matrix was normalized to 10,000/cell by the total UMI count per cell and then log-transformed by adding one and standardizing for each gene using *scanpy.pp.normalized_total(target_sum=1e4)* and *scanpy.pp.log1p.* Then, highly variable genes were selected based

on specific thresholds for mean expression and dispersion using *scanpy.pp.highly_variable_genes* (min_mean=0.0125, max_mean=3, min_disp=0.5). We conducted and visualized Uniform Manifold Approximation and Projection (UMAP) embeddings of the latent cell states of a single cell. The major cell types were annotated by comparing the canonical marker genes and the differentially expressed genes (DEGs) for each cluster.

2.4 | Spatial transcriptomic data processing

We downloaded the raw count matrix data from a spatial transcriptomic dataset (10x Genomics) for 3313 spots from a patient (ST-P1) who did not receive neoadjuvant chemotherapy treatment. The Python package *Scanpy* (v1.9.3) was used for processing. We filtered according to the following criteria: <20% mitochondrial gene expression in UMI counts and genes detected in at least 10 of the total spots. The count matrix was normalized and then log-transformed using *scanpy.pp.normalize_total* and *scanpy.pp.log1p*.

2.5 | DEG enrichment analysis

Cluster-based detection of DEGs was performed using the Wilcoxon rank-sum test and Benjamini–Hochberg method[22] to correct for multiple comparisons (*scanpy.tl_rank_genes_groups*). DEGs with an adjusted *p*-value <0.01 and log2 fold change >0.5 were evaluated. Gene ontology and Reactome pathway analyses of the DEGs were performed using the Python package *gseapy* (v1.0.4).

2.6 | Cell lines and cell culture

The human CRC cell lines Colo320 and SW480 cells were obtained from the Japanese Collection of Research Bioresources Cell Bank; HT29, LS174T, and RKO cells were obtained from ATCC; SW620 cells were obtained from KAC. All cell lines were cultured in an appropriate medium supplemented with 10% FBS with 1% antibiotic/antimycotic solution (Thermo Fisher Scientific). All cells were maintained in a humidified atmosphere at 37°C in an atmosphere containing 5% CO_2. Cell cultures were tested for mycoplasma infection using Myco Alert (Lonza, Walkersville, MD, USA) according to the manufacturer's protocol.

2.7 | RNA extraction and reverse-transcription quantitative polymerase chain reaction

Total RNA was extracted from frozen tissue specimens and cell lines using ISOGEN-II (Nippon Gene) and the AllPrep DNA/RNA Mini kit (QIAGEN), and reverse-transcription quantitative

polymerase chain reaction (RT-qPCR) was performed as described previously.[23] The mRNA levels were normalized to that of 18S mRNA, as an internal control, and expressed relative to the level of the cDNA from the Human Universal Reference Total RNA (Clontech). We analyzed the statistical significance of mRNA expression levels using experimental triplicates. Gene expression was quantified using the following oligonucleotide primers: BRD3: 5′-ATCATCCAATCTCGGGAGCC-3′ (sense) and 5′-CCTGTTTCTTCCCGCTTGC-3′ (antisense), BRD4: 5′-CTTTGA GACCCTGAAGCCGTC-3′ (sense) and 5′-GAAACCAGCGAAGC ATCTCCC-3′ (antisense), p21: 5′-TGTCCGTCAGAACCCATGC-3′ (sense) and 5′- AAAGTCGAAGTTCCATCGCTC-3′ (antisense), and 18s: 5′-AGTCCCTGCCCTTTGTACACA-3′ (sense) and 5′-CGATCC GAGGGCCTCACTA-3′ (antisense).

2.8 | Immunohistochemical analysis

Immunohistochemical analysis of CRC tissue samples and tissue specimens from mouse xenograft tumors was performed as described previously.[24] All sections were counterstained with hematoxylin. The following primary antibodies were used: anti-BRD3 (1:200, 11859-1-AP, Proteintech), anti-BRD4 (1:200, ab128874, Abcam), and anti-p21 (1:50, #2947, Cell Signaling Technologies). p21 scores were determined by observing the most intensely stained areas. Tumor histology was independently performed by an experienced research pathologist at Kyusyu University Beppu Hospital.

2.9 | Small interfering RNA-mediated knockdown

BRD3 siRNA (#s15544, #s15545), *BRD4* siRNA (#s23901, #s23902), and negative control siRNA were purchased from Thermo Fisher. Transfection of CRC cells with siRNA oligonucleotides was performed using Lipofectamine RNAiMAX (Thermo Fisher) as described previously.[25]

2.10 | Transient overexpression of BRD3 by transfection and generation of Colo320/SW620 cells stably overexpressing BRD3

The BRD3-expressing lentiviral plasmid vector (pLV [Exp]-Puro-CMV > hBRD3[NM_007371.4]) and empty plasmid vector (pLV [Exp]-Puro-CMV > ORF_Stuffer) as the control were purchased from VectorBuilder. In transient overexpressing analysis, we transfected the plasmid vectors for CRC cells using Lipofectamine 3000 (Thermo Fisher Scientific) following the manufacturer's protocol. To generate stably overexpressing CRC cells, lentiviruses were produced in 293FT cells using the Vira Power Lentiviral packing mix (Thermo Fisher Scientific), and the supernatant was collected 48h after transfection. Colo320 and SW620 cells were infected

with the lentiviral supernatant and then selected with puromycin. Control cells were generated by transfecting cells with an empty vector with ORF_Stuffer.

2.11 | Protein extraction

Total proteins were collected as described previously.[26] Nuclear proteins were collected using the EPIXTRACT Nuclear Protein Isolation Kit (ENZ-45016, Enzo Life Sciences, Ann Arbor, MI, USA) according to the manufacturer's instructions.

2.12 | Western blot analysis

Western blot analysis was performed as described previously.[26] The following antigen-specific primary antibodies were used: rabbit polyclonal antibody against BRD3 (1:1000, Proteintech), rabbit monoclonal antibody against BRD4 (1: 2000, Abcam), the mixture of three specific rabbit monoclonal antibodies against phosphor-cdk2 Tyr15, phosphor-histone H3 Ser10, and β-actin (1:250, ab136810, Abcam), rabbit polyclonal antibody against Lamin B1 (1:5000, 12987-1-AP, Proteintech), and mouse monoclonal antibody against β-actin (1:1000, Santa Cruz Biotechnology).

2.13 | Colony formation assay

Colony formation assays were performed according to standard protocols, as described previously.[27] For *BRD3* knockdown studies, cells were plated at a density of 1000 cells/well (Colo320) or 500 cells/well (HT29) in triplicate in 6-well plates and transfected with *BRD3* siRNA or negative control siRNA. For BRD3 overexpression studies, cells were plated at a density of 2500 cells/well (Colo320) or 1500 cells/well (SW620) in triplicate in a 6-well plate and transfected with a BRD3-expressing lentiviral vector or control vector. For the *BRD4* knockdown studies, cells were plated at a density of 2000 cells/well (Colo320) or 300 cells/well (HT29) in triplicate in 6-well plates and transfected with *BRD4* siRNA or negative control siRNA. For the BRD3 overexpression combined with *BRD4* knockdown studies, cells were plated at a density of 2000 cells/well (Colo320) or 1500 cells/well (SW620) in triplicate in 6-well plates and transfected with *BRD4* siRNA or negative control siRNA. After 10–14 days, visible colonies were photographed using the FUSION SOLO S imaging system (VILBER). Colony counts were determined using ImageJ software (v1.80; NIH).

2.14 | Cell cycle assay

Cells were synchronized at the G1 phase of the cell cycle via serum starvation for 96 h and restimulated by changing the medium to that containing 10% FBS. Cell cycle assays were performed as described previously.[28] The cell cycle distribution was measured using the SH800 cell sorter (Sony Biotechnology).

2.15 | Murine xenograft model

All animal procedures were performed in compliance with the Guidelines for the Care and Use of Experimental Animals established by the Committee for Animal Experimentation of Kyusyu University. Subcutaneous murine xenografts were analyzed as described previously.[27] Four-week-old female BALB/c nu/nu mice were purchased from Japan SLC and maintained under specific pathogen-free conditions. For subcutaneous xenograft assays, 1×10^6 control cells or BRD3-overexpressing SW620 cells were suspended in 100 μL 50% Matrigel (Corning) in PBS and injected bilaterally into nude mice. Tumor size was calculated using the following formula: tumor volume = length × width^2 × 0.5.

2.16 | Statistical analysis

Associations between variables were analyzed using Welch's *t*-test and the Mann–Whitney U test. The degree of linearity was assessed using Pearson's correlation coefficient. The statistical analyses were performed using R software v4.2.0 and Python v3.9.16. A two-sided *p*-value <0.05 was deemed statistically significant.

3 | RESULTS

3.1 | BRD3 inhibits CRC tumor growth in vitro and in vivo

Changes in the proliferation of CRC cell lines after *BRD3* knockdown or overexpression were examined using the colony formation assay. We used Colo320 and HT29 cell lines for *BRD3* knockdown and overexpression analysis, and SW620 cell lines used for BRD3 overexpression analysis because of their low expression levels of BRD3 (Figure S1). Significant downregulation of *BRD3* mRNA and protein expression was confirmed in *BRD3*-knockdown cells (Figure 1A). *BRD3* knockdown increased the proliferation of CRC cells (Figure 1B), whereas BRD3 transient overexpression inhibited the proliferation of CRC cells (Figure 1C,D).

Next, we conducted an in vivo analysis using SW620 cells with stable overexpression of BRD3 (Figure 1E). BRD3 overexpression significantly decreased the volume of CRC tumors in mouse models (Figure 1F). RT-qPCR and immunohistochemical analysis showed stronger BRD3 expression in xenograft tumors derived from BRD3-overexpressing SW620 cells compared with control cells (Figure 1G).

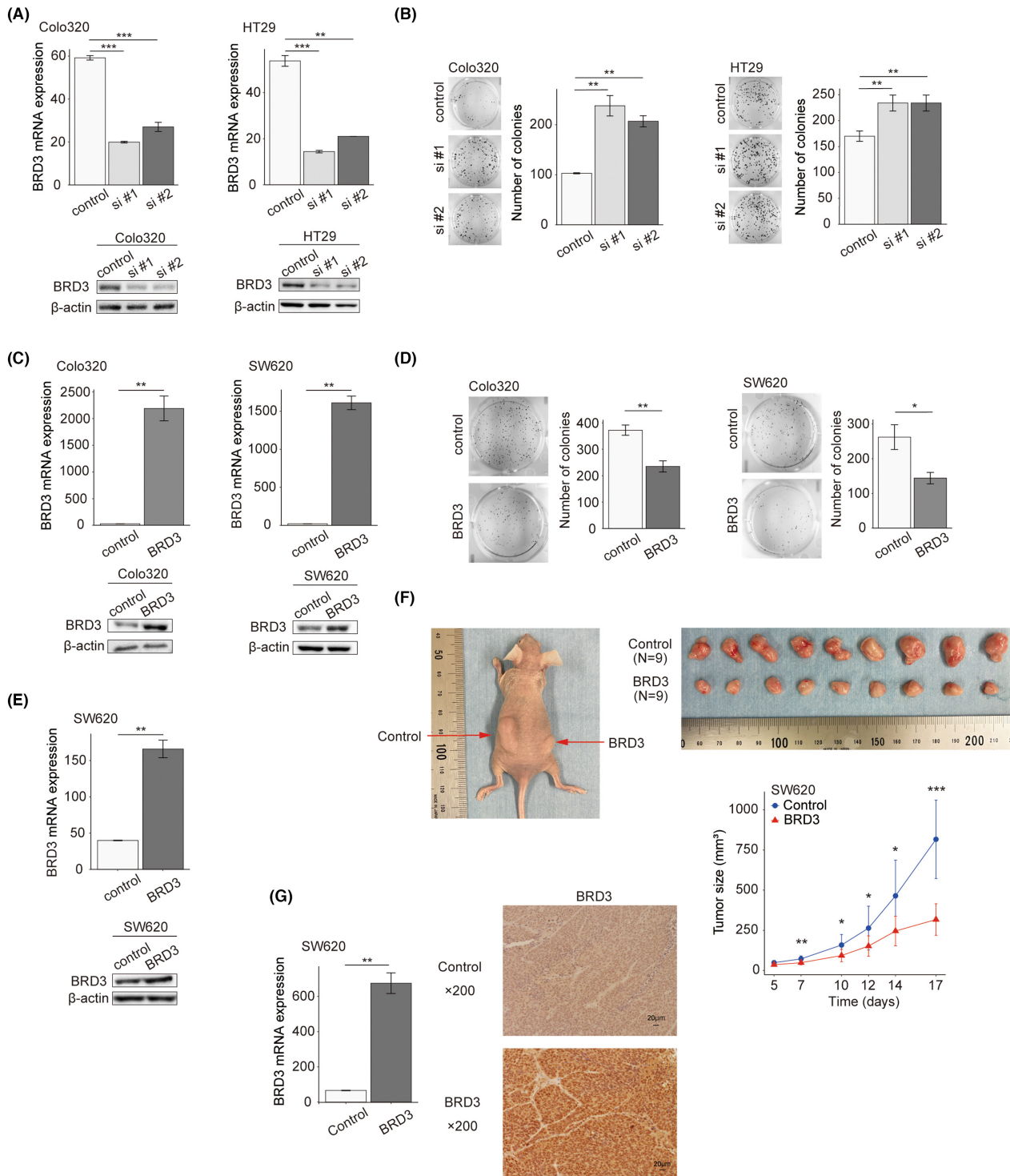These results suggest that BRD3 inhibits CRC tumor growth.

FIGURE 1 Effects of *BRD3* knockdown and overexpression on cell proliferation in colorectal cancer (CRC) cells in vitro and in vivo. (A) *BRD3* mRNA expression normalized to 18S expression according to reverse-transcription quantitative PCR (RT-qPCR) and protein expression according to western blot analysis (WB) in *BRD3*-knockdown and control CRC cells. **$p < 0.01$; ***$p < 0.001$. (B) Colony formation assays using *BRD3*-knockdown CRC cells. **$p < 0.01$. (C) *BRD3* mRNA expression normalized to 18S expression according to RT-qPCR and protein expression according to WB in BRD3 transiently overexpressing and control CRC cells. **$p < 0.01$. (D) Colony formation assays using BRD3 transiently overexpressing CRC cells. *$p < 0.05$; **$p < 0.01$. (E) *BRD3* mRNA expression normalized to 18S expression according to RT-qPCR (left) and protein expression according to WB (right) in CRC cells with stable BRD3 overexpression and control CRC cells. **$p < 0.01$. (F) In vivo analysis using a murine xenograft model. Size of tumors derived from CRC cells with stable BRD3 overexpression and control CRC cells. $N = 9$ per group. *$p < 0.05$; **$p < 0.01$; ***$p < 0.001$. (G) *BRD3* mRNA expression normalized to 18S expression according to RT-qPCR (left) and immunohistochemical staining of BRD3 (right) in tumors derived from CRC cells with stable BRD3 overexpression and control CRC cells. **$p < 0.01$. Scale bars, 20 μm; original magnification, ×200.

3.2 | BRD3 prevents cell cycle progression from the G1 to S phase in CRC cells

To determine whether BRD3 prevents cell cycle progression, we performed a western blot analysis. Cyclin-dependent kinase 2 (Cdk2) is inactivated in the G1/S phase via phosphorylation of Tyr15. The protein expression of Cdk2pTyr15 was suppressed in *BRD3*-knockdown cells and elevated in BRD3 transiently overexpressing cells (Figure 2A).

Next, we performed cell cycle analysis using Colo320 cells with stable overexpression of BRD3 (Figure 2B). Compared with control cells, BRD3-overexpressing cells had a lower proportion of cells in the S phase after restimulation with medium containing 10% FBS (Figure 2C).

These results suggest that BRD3 overexpression halts cell cycle progression from the G1 to the S phase.

3.3 | Regulation of p21 expression by BRD3

We showed that BRD3 inhibits the transition from G1 to S phase by cell cycle analysis. It has been reported that BRD4 regulates the expression of p21, which is involved in G1/S arrest, in that *BRD4* knockdown and a pan-BET inhibitor (JQ1) upregulated p21 expression.[29–31] Public ChIP-seq data using a human multiple myeloma cell line (GSE43743) showed that BRD3 co-occupied with BRD4 near the transcription start site (TSS) of p21 (Figure S2). Based on those findings, we hypothesized that BRD3 also regulates p21 expression. We found that *BRD3* knockdown significantly decreased *p21* mRNA expression in CRC cells, while the *BRD4* expression level did not change (Figures 3A and S3A). In addition, BRD3 transient overexpression increased *p21* mRNA expression with slight upregulation of *BRD4* mRNA (Figures 3B and S3B). Furthermore, in western blot analysis, the expression of p21 was decreased in *BRD3*-knockdown cells and was increased in BRD3 transiently overexpressing cells (Figure 3C). Similarly, RT-qPCR and immunohistochemical analysis of murine xenograft models showed significantly greater p21 expression in tumor tissues derived from SW620 cells with stable overexpression of BRD3 than controls, while there was no difference in BRD4 expression (Figure 3D,E).

These results suggest that BRD3 could upregulate p21 expression without affecting BRD4 expression in CRC cells.

3.4 | BRD3 expression is upregulated in CRC patients

Next, we focused on the expression of BET family genes (*BRD2*, *BRD3*, *BRD4*, *BRDT*) in CRC patients. In TCGA data, *BRD2*, *BRD3*, and *BRD4* mRNA levels were higher in tumor tissues than in normal tissues (Figure 4A). Our CRC cohort also showed higher *BRD3* and *BRD4* mRNA expression in tumor tissues (Figure 4B). *BRD3* mRNA expression was most positively correlated with *BRD4* mRNA expression among the BET family genes in TCGA data, our CRC cohort data, and a public CRC organoid dataset (Figures 4C,D and S4).

In our immunohistochemical analysis, BRD3 staining was more intense in the nucleus of CRC cells than in normal colon epithelial cells. In addition, BRD4 staining was also more intense in BRD3 high-expression regions (Figure 4E).

These results indicate that not only BRD4 but also BRD3 is overexpressed in CRC cells, and BRD3 expression is correlated most strongly with BRD4 expression among the BET family genes.

3.5 | scRNA-seq analysis of CRC tissues

We evaluated *BRD3* expression in CRC tissues using public CRC scRNA-seq data (3 patients, 44,020 cells).[32] Six cell types were annotated with marker genes (Figures 5A and S5A). Among these cells, cell groups from carcinoma cells were extracted (Figures 5B and S5A). *BRD3* was particularly highly expressed in epithelial cells, as were *BRD2* and *BRD4* (Figures 5C,D and S5B). We divided the carcinoma epithelial cells into two groups at the median value of *BRD3* mRNA expression ($p < 0.001$, $\log_2$ fold change $= 29.7$) (Figure 5E). *BRD2* and *BRD4* were expressed in both two groups (Figure S5C). In the *BRD3*-high-expression group, cell cycle and cell cycle checkpoints-related pathways were enriched in Reactome pathway and gene ontology biological process (Figures 5F and S5D).

This analysis indicates that BRD3 is expressed in epithelial cells in tumor tissues and BRD3 high expressed cells are associated with cell cycle-related pathways in CRC.

3.6 | Spatial transcriptomic analyses of CRC tissues

To examine the relationship between spatial *BRD3* expression and *BRD4/p21* expression in CRC tissues, we performed spatial transcriptomic analysis using previously published CRC data[33] (Figure 6A). First, the spatial expression of *BRD3*, *BRD4* and *p21* was confirmed (Figure 6B). We divided the spots into two groups based on the median *BRD3* mRNA level ($p < 0.001$, $\log_2$ fold change $= 30.2$) (Figure 6C). *BRD4* expression was not significantly different between the high and low *BRD3* expression groups, but *p21* expression was significantly higher in the high *BRD3* expression group ($p < 0.05$, $\log_2$ fold change $= 0.17$) (Figure 6D). Conversely, when the spots were divided according to the median *BRD4* mRNA level ($p < 0.001$, $\log_2$ fold change $= 3.4$), there was no significant difference in *BRD3* or *p21* expression (Figure S6). Gene set enrichment analysis showed that cell cycle checkpoint pathways were enriched in the high *BRD3* expression group (Figure 6E). Furthermore, in the publicly available CRC scRNA-seq data described above, *p21* expression was significantly higher in the cells with high *BRD3* expression ($p < 0.001$, $\log_2$ fold change $= 0.18$) (Figure 6F).

These analyses of CRC indicate that BRD3 expression is positively correlated with p21 expression and is significantly associated with cell cycle checkpoint pathways. These results are consistent with our findings in CRC cells.
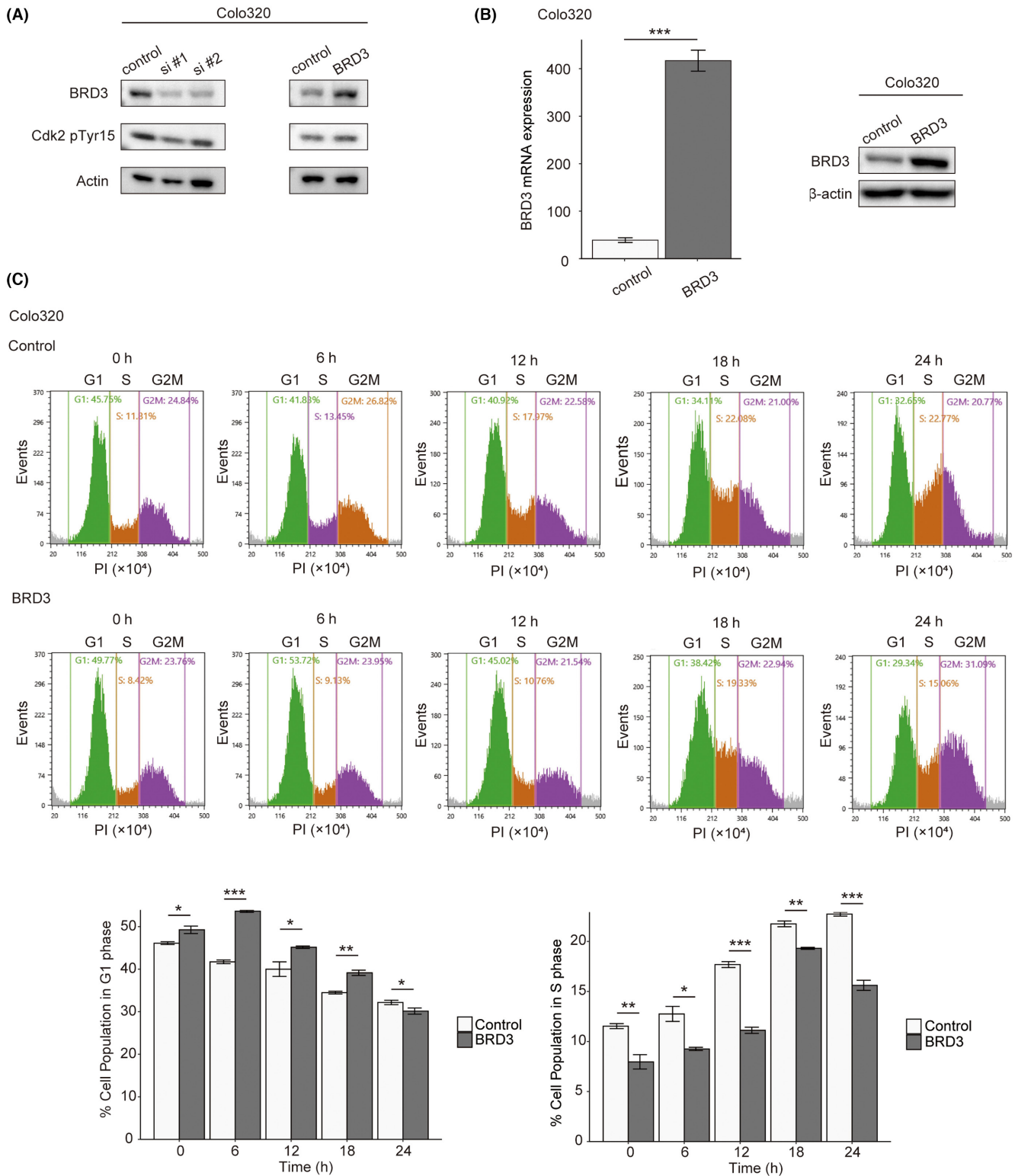
FIGURE 2 Cell cycle progression halted by BRD3 from the G1 to the S phase in colorectal cancer (CRC) cells. (A) Protein expression using western blot analysis (WB) for BRD3 and Cdk2 pTyr15 in *BRD3*-knockdown (left) and transiently overexpressing (right) CRC cells. (B) *BRD3* mRNA expression normalized to 18S expression according to RT-qPCR (left), and protein expression according to WB (right) in CRC cells with BRD3 stable overexpression and control CRC cells. ***$p < 0.001$. (C) Cell cycle analysis by flow cytometry after stimulation with FBS in CRC cells with BRD3 stable overexpression and control CRC cells. *$p < 0.05$; **$p < 0.01$; ***$p < 0.001$.
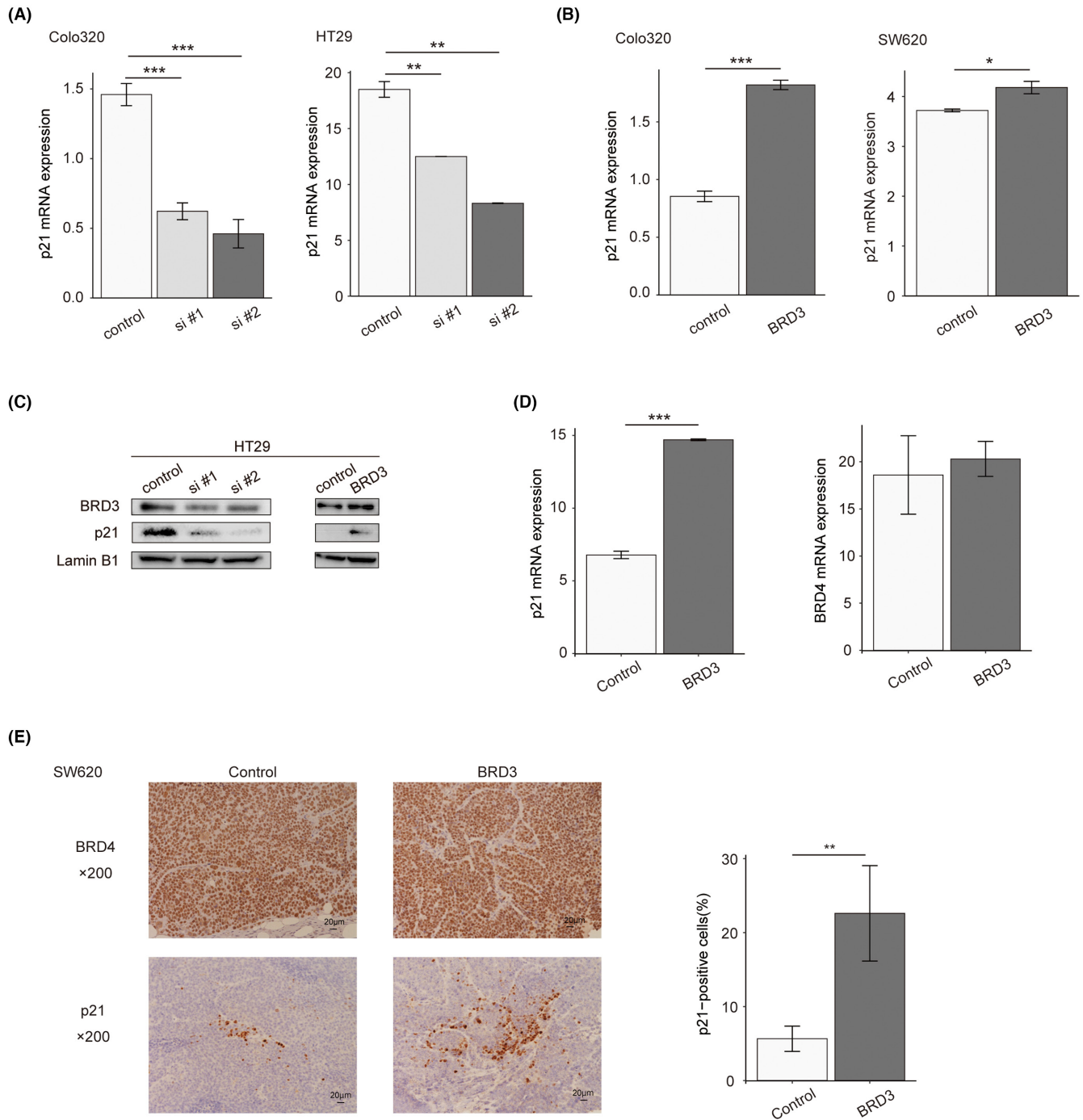
FIGURE 3 Upregulated p21 expression by BRD3 in colorectal cancer (CRC) cells. (A) *p21* mRNA expression normalized to 18S expression according to reverse-transcription quantitative PCR (RT-qPCR) in *BRD3*-knockdown and control CRC cells. **p < 0.01; ***p < 0.001. (B) *p21* mRNA expression normalized to 18S expression according to RT-qPCR in BRD3 transiently overexpressing and control CRC cells. *p < 0.05; ***p < 0.001. (C) Protein expression using western blot analysis (WB) for BRD3, p21, LaminB1 in *BRD3*-knockdown (left) and transiently overexpressing (right) CRC cells. (D) *p21* and *BRD4* mRNA expression normalized to 18S expression according to RT-qPCR in tumor tissues derived from CRC cells with BRD3 stable overexpression and in those derived from control CRC cells. ***p < 0.001. (E) Immunohistochemical staining of BRD4 or p21 in tumor tissues derived from CRC cells with BRD3 stable overexpression and in those derived from control CRC cells. Scale bars, 20 μm; original magnification, ×200. p21 scores were determined by observing the most intensely stained areas. **p < 0.01.

3.7 | BRD3 overexpression inhibits the proliferation of *BRD4*-knockdown CRC cells

BRD4 is reported to be a driver gene that contributes to tumor cell growth,[13] and the inhibition of BRD4 could suppress tumor growth.[11,34] To investigate whether BRD3 overexpression is a potential therapeutic target, we evaluated the proliferation of CRC cells with BRD3 stable overexpression and control CRC cells after *BRD4* knockdown. Significant downregulation of *BRD4* mRNA and protein expression was observed in *BRD4*-knockdown cells (Figure 7A).
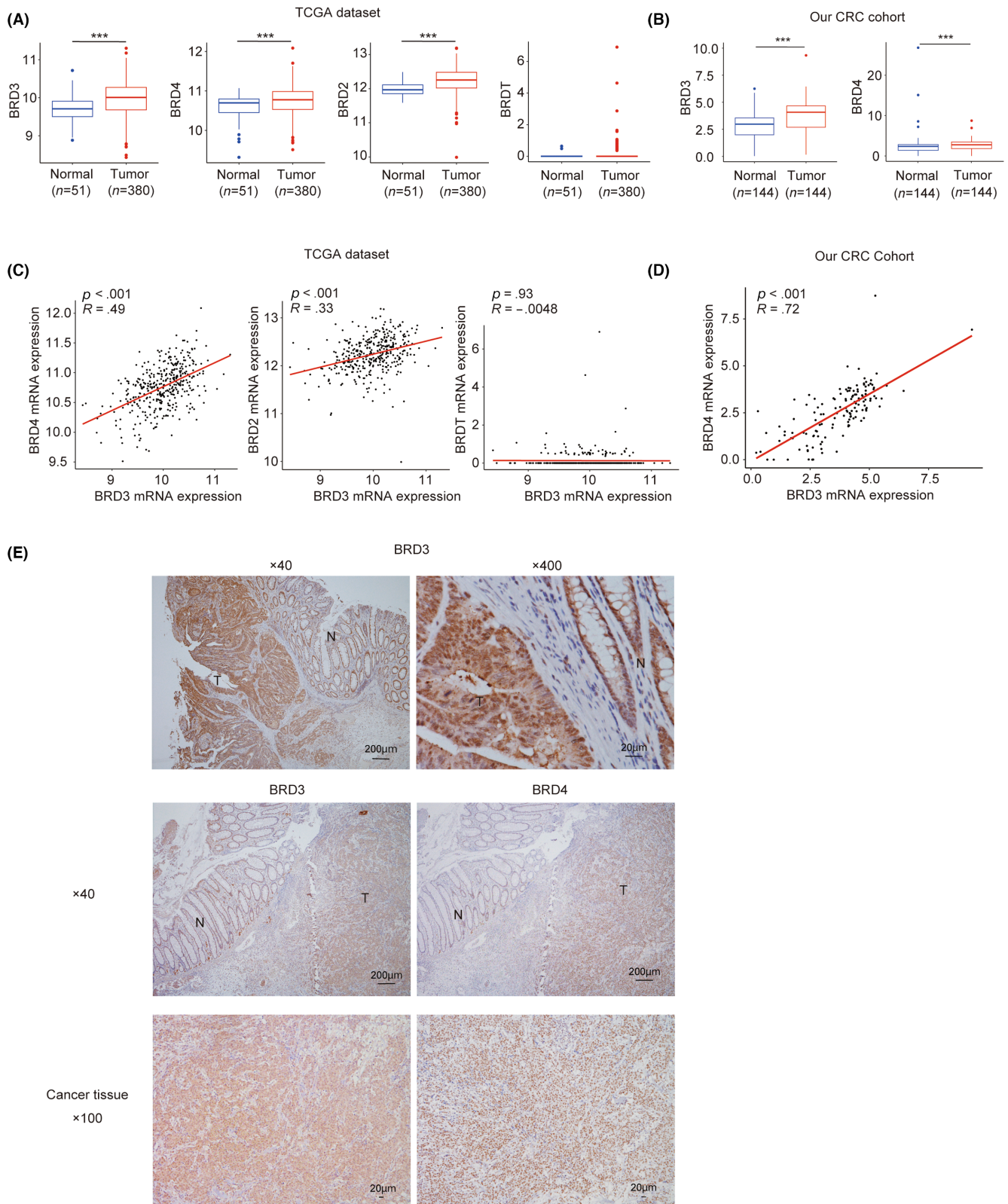
FIGURE 4 Expression of BET family genes and correlations between *BRD3* and other BET gene expression levels in colorectal cancer (CRC). (A) mRNA expression of BET family genes (*BRD3, BRD2, BRD4, BRDT*) in 380 CRC tissues and 51 normal colon tissues obtained from The Cancer Genome Atlas (TCGA) dataset. ***$p < 0.001$. (B) *BRD3* and *BRD4* mRNA expression according to reverse-transcription quantitative PCR in 144 CRC tissues and paired normal colon tissues in our CRC cohort dataset. ***$p < 0.001$. (C, D) Correlation between the mRNA expression of *BRD3* and that of other BET genes in TCGA dataset (A) and our CRC cohort (B). *R* indicates the Pearson correlation coefficient. (E) Immunohistochemical staining of BRD3 and BRD4. Upper: scale bar, 200 μm (left) and 20 μm (right). Original magnification, ×40 (left) and ×400 (right). Lower: scale bar, 200 μm (upper) and 20 μm (lower). N, normal tissue; T, tumor tissue.
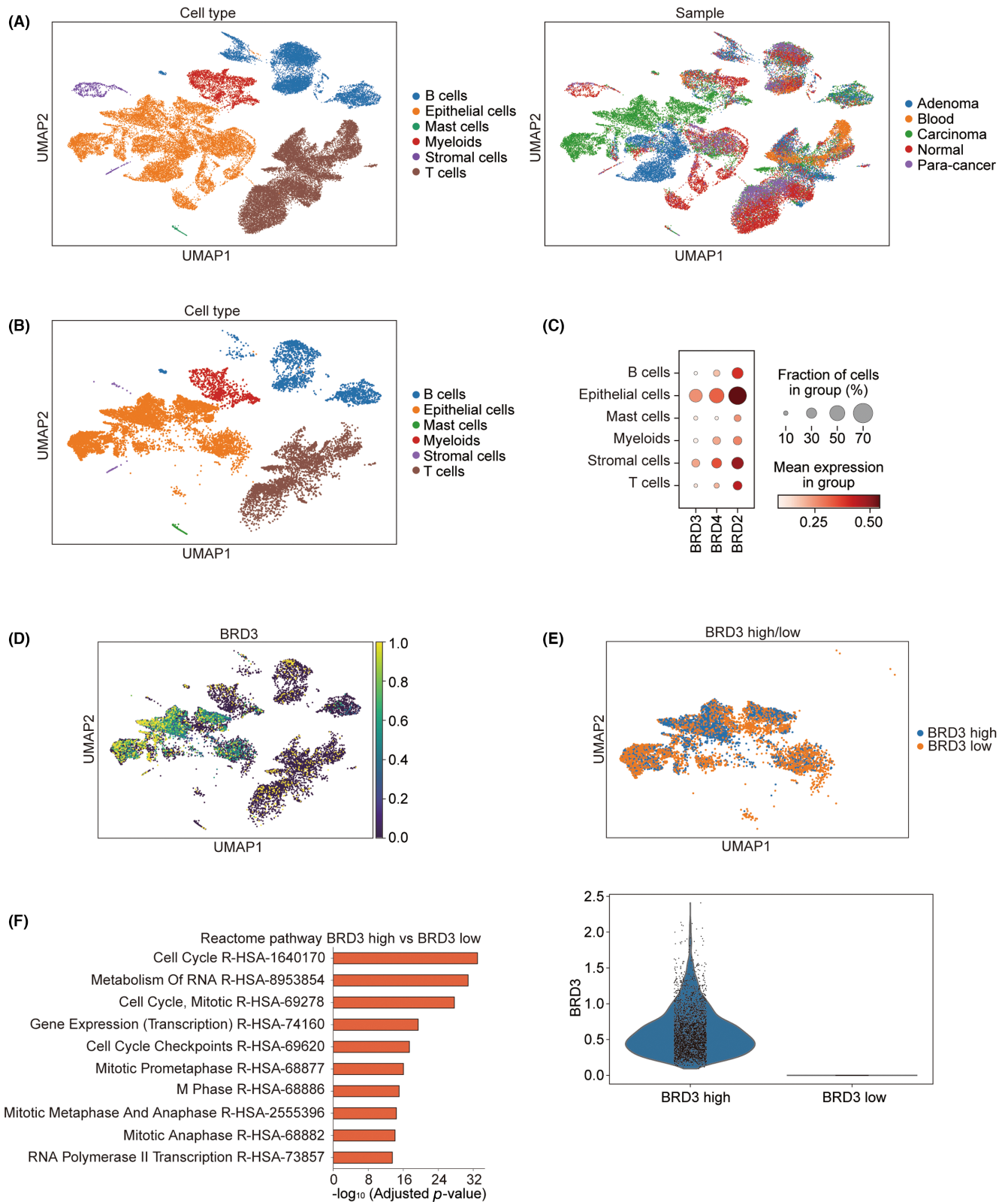
FIGURE 5 *BRD3* expression and enrichment pathway analysis in single-cell colorectal cancer (CRC) data. (A) Uniform Manifold Approximation and Projection (UMAP) of cell types in all cells (left) and tissues (right). (B) UMAP of cell types after annotation of carcinoma cells. (C) Dot plot of the expression and expression proportions of *BRD3*, *BRD4*, and *BRD2* per cell type. The circle size represents the cell proportion. (D) Expression of *BRD3* in UMAP representations. (E) Upper: UMAP distribution in carcinoma epithelial cells with high versus low *BRD3* expression. Lower: violin plots of *BRD3* expression in high versus low *BRD3* mRNA expression groups (divided by the median *BRD3* mRNA level). (F) Reactome pathway analysis of carcinoma epithelial cells with high versus low *BRD3* expression.
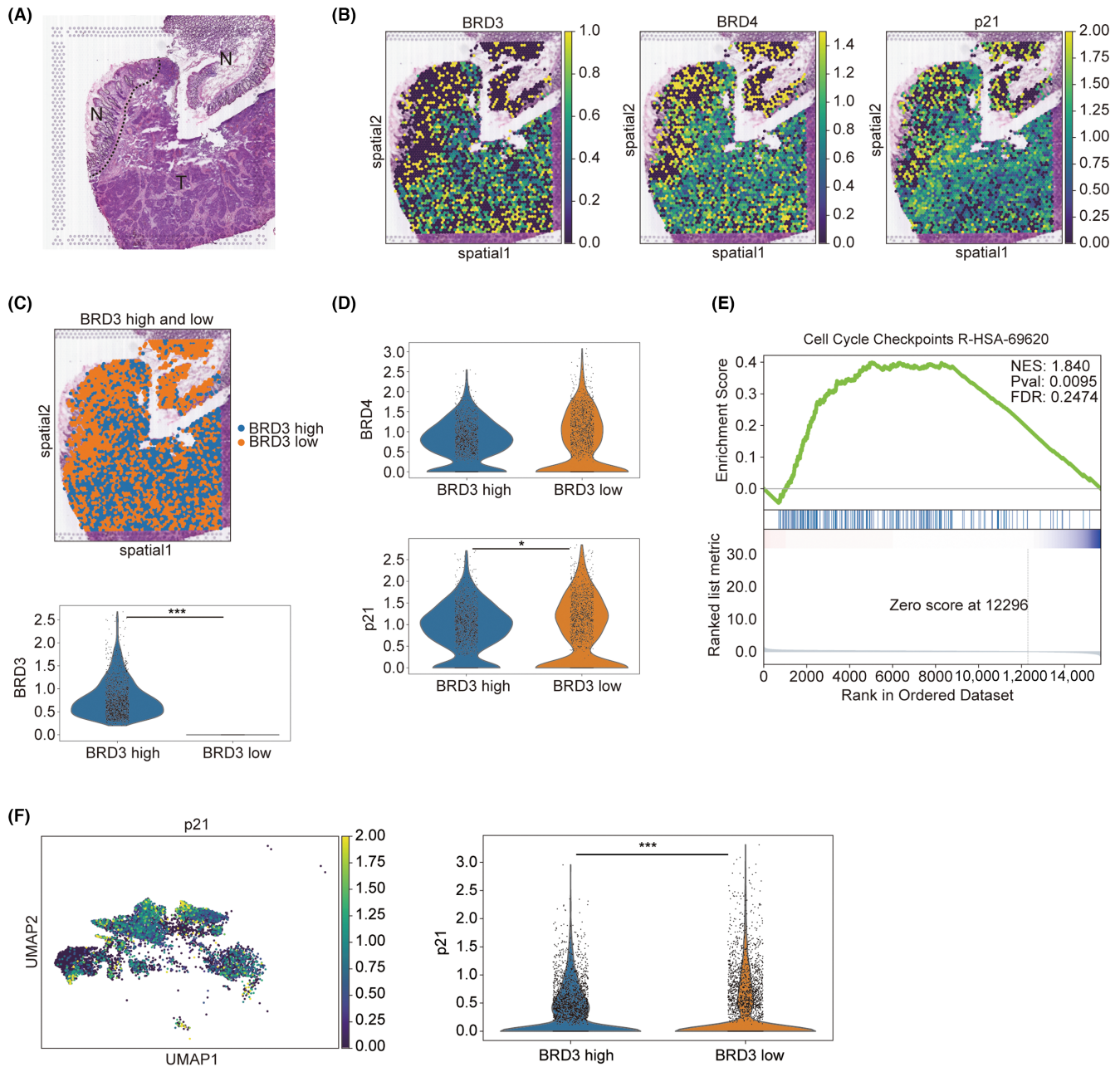
FIGURE 6 Spatial transcriptomic and single-cell analysis revealing a positive correlation between *BRD3* and *p21* expression in colorectal cancer (CRC). (A) Pathological diagnosis in colorectal tissue in a tissue slide used for spatial transcriptomic analysis. Normal: normal tissue; Tumor: tumor tissue. (B) Spatial distribution of *BRD3*, *BRD4*, and *p21* expression. (C) Upper: spatial distribution in tissue regions with high versus low *BRD3* expression. Lower: violin plots of *BRD3* expression in high versus low *BRD3* mRNA expression groups (divided by the median *BRD3* mRNA level). ***$p < 0.001$. (D) Violin plots of *BRD4* and *p21* expression in the high versus low *BRD3* mRNA expression groups. *$p < 0.05$. (E) Gene set enrichment analysis of tissue regions with high versus low *BRD3* expression. Pval, *p*-value; FDR, false discovery rate; NES, normalized enrichment score. (F) *p21* expression in Uniform Manifold Approximation and Projection (UMAP) representations of carcinoma epithelial cells based on scRNA-seq data (left), and violin plots of *p21* expression in the high versus low *BRD3* mRNA expression groups (right). ***$p < 0.001$.

Colony formation assays showed that the proliferation of CRC cell lines was inhibited by *BRD4* knockdown, as reported elsewhere[11,34] (Figure 7B). Notably, BRD3 overexpression had an additive inhibitory effect on the cell growth under *BRD4* knockdown (Figure 7C).

These results suggest that overexpression of BRD3 as well as inhibition of BRD4 could be a potential therapeutic approach in CRC, and combining BRD3 activation with BRD4 inhibition may be an effective strategy for CRC patients.

4 | DISCUSSION

In this study, we examined the association of the epigenetic regulator BRD3 with tumor progression using in vitro and in vivo analyses with CRC cells and scRNA-seq and spatial transcriptomics in CRC tumor tissues. To the best of our knowledge, this report is the first to describe the tumor suppressive function of BRD3 possibly via promotion of p21 expression in CRC.
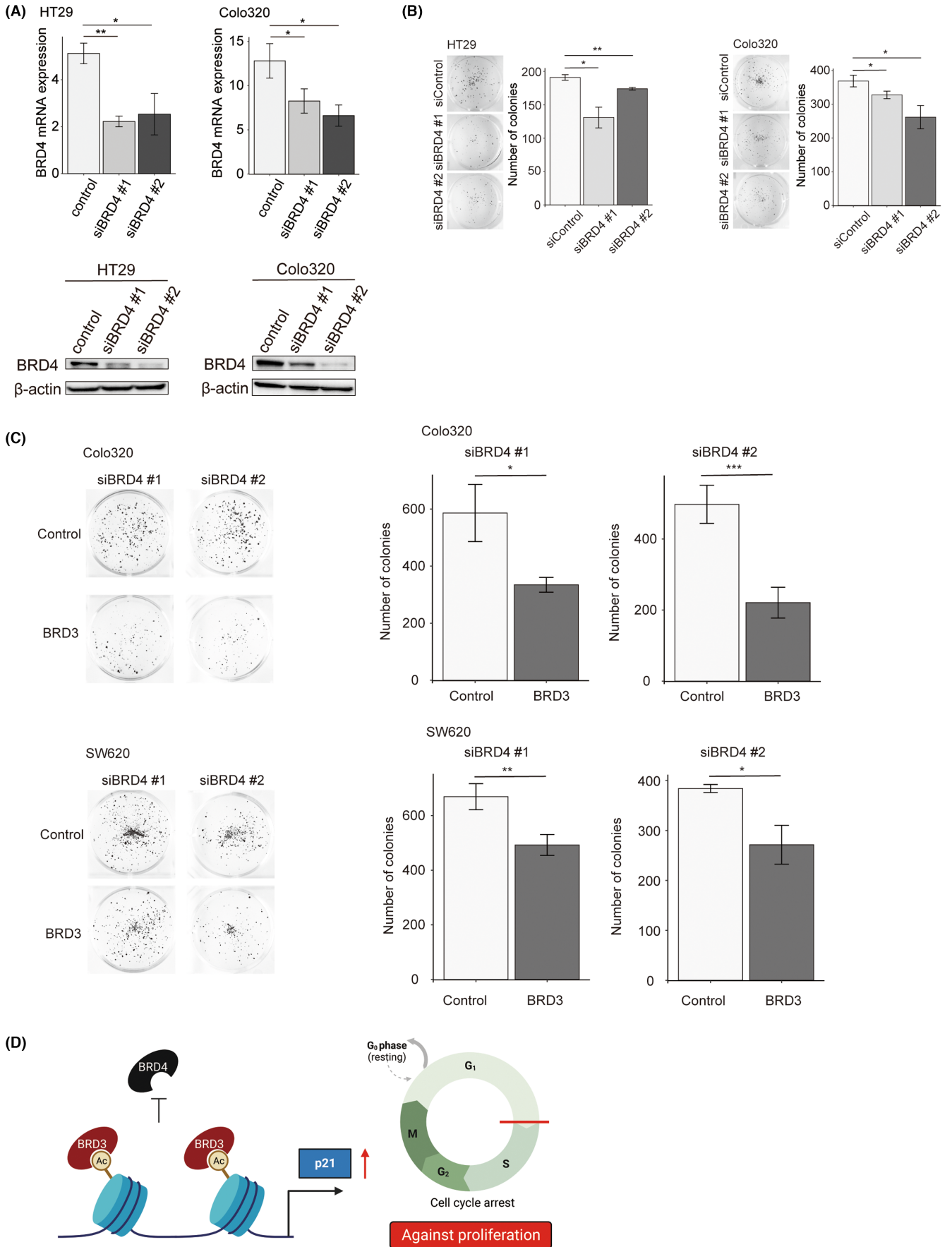
FIGURE 7 Tumor growth inhibited by BRD3 overexpression in *BRD4*-knockdown colorectal cancer (CRC) cells. (A) *BRD4* mRNA expression normalized to 18S expression according to reverse-transcription quantitative PCR (RT-qPCR) (upper) and protein expression according to western blot analysis (WB) (lower) in *BRD4*-knockdown and control CRC cells. $*p < 0.05$; $**p < 0.01$. (B) Colony formation assays using *BRD4*-knockdown cells. $*p < 0.05$. $**p < 0.01$. (C) Colony formation assays after *BRD4* knockdown in CRC cells with BRD3 stable overexpression and control CRC cells. $*p < 0.05$; $**p < 0.01$; $***p < 0.001$. (D) Summary of the results. BRD3 inhibits proliferation of CRC cells by suppressing cell cycle progression possibly via promoting p21 expression.

Our cellular analyses using BRD3-overexpressing or *BRD3*-knockdown CRC cells and expression analyses using scRNA-seq and spatial transcriptomics in CRC tissues showed that BRD3 suppressed cell proliferation by inhibiting cell cycle progression. Furthermore, BRD3 inhibited G1/S transition by inducing expression of p21, a cell cycle checkpoint protein (Figure 7D). However, how BRD3 regulates p21 expression remains unknown. BRD4 has been reported to suppress p21 expression via FOXO1 or miR-106b.[29,30] BRD3 expression reduces BRD4 occupancy at the transcriptional start site of genes, where BRD4 binds to and depletes ribosomal RNA. Moreover, high levels of BRD3 antagonize BRD4 by inhibiting the binding of other BETs to BDs and competing for binding to common loci.[18] We also showed BRD3 and BRD4 occupancy at common loci near the TSS of p21 in ChIP-seq data analysis in a human multiple myeloma cell. These findings suggest that BRD3 could antagonize BRD4 subsequent to upregulation of p21 expression, leading to inhibition of tumor proliferation. Further investigation is required to clarify the molecular mechanism underlying the tumor-suppressive role of BRD3 in CRC.

Pan-BET inhibitors are currently in clinical trials worldwide for clinical use.[35] Pan-BET inhibitors inhibit the interaction between BET proteins and chromatin by displacing BET proteins from acetylated lysine residues on histones by binding to the BDs of BET proteins, failing to activate proteins involved in transcriptional regulation of driver genes such as MYC, BCL2, and CDK6.[2,6] Models of many other cancers, including acute myeloid leukemia, medulloblastoma, breast cancer, lung cancer and CRC, showed an anti-tumorigenic response to the pan-BET inhibitor JQ1.[36–39] However, drug resistance to pan-BET inhibitors has been reported in various cancers.[36–42] The lack of selectivity of pan-BET inhibitors is considered to influence the antitumor effect of, and drug resistance to, BET inhibitors. Thus, selective inhibition of individual BET genes, such as via BRD-degrading proteolysis-targeting chimera, is a potential approach to targeting specific BET family proteins.[43] In CRC, the selective BRD4 degrader A1874 is more effective than known pan-BET inhibitors, including JQ1.[44] However, selective inhibitors or activators of other BET family members have not been developed. Here, we demonstrated that BRD3 overexpression under BRD4 inhibition strongly inhibited tumor proliferation. These results suggest that BRD3 inhibition may cause pan-BET inhibitor resistance. Thus, combining a BRD3 analog with selective BRD4 inhibitors might be a promising therapeutic approach for CRC.

Interestingly, our clinical analysis showed that BRD3, as well as BRD4, was highly expressed in tumor tissues compared with normal tissues, even though BRD3 was found to have a tumor-suppressive role in CRC. This discrepancy may be due to the compensatory upregulation of BRD3 against driver genes, similar to tumor suppressor genes such as p73 and p16, as described elsewhere.[45–47] As expected, BRD3 expression was positively correlated with BRD4 expression in CRC tissues. Thus, high expression of BRD3 in tumor tissues could be the result of compensatory upregulation against driver genes such as BRD4. Further study will be required to elucidate the regulatory mechanism of BRD3 expression in CRC.

In this study, we demonstrated that BRD3, a BET family gene, has a tumor-suppressive role by preventing tumor growth, possibly via cell cycle inhibition by regulating p21 expression. Activation of BRD3 may be a potential therapeutic approach targeting epigenetic regulators in CRC.

23ck0106825h001, 23ck0106800h001, 22ama221501h0001, 21ck0106690s0201, 20cm0106475h0001, 20ck0106547h0001, and 20ck0106541h0001); Takeda Science Foundation; and The Princess Takamatsu Cancer Research Fund. Figure 7D was created using bioRENDER (https://app.biorender.com/).

CONFLICT OF INTEREST STATEMENT

Koshi Mimori is an editorial board member of *Cancer Science* and other authors have no conflicts of interest to disclose.

ETHICS STATEMENT

Approval of the study protocol by an institutional review board: the study was approved by the Kyushu University Institutional Review Board (approval #22185−00) and was performed in accordance with the tenets of the Declaration of Helsinki.

Informed consent: informed consent was obtained in the form of opt-out on the website (https://www.beppu.kyushu-u.ac.jp/geka/information/clinical_disclosure/). Those who opted out were excluded.

Registry and registration no. of the study/trial: N/A.

Animal studies: the experimental protocols were approved by the Animal Care and Use Committee of Kyushu University (approval A22-405-0), and the experiments were conducted in accordance with the institutional ethical guidelines for animal experiments and the safety guidelines for gene manipulation experiments.

ORCID

Masahiro Hashimoto https://orcid.org/0000-0002-9264-6057
Takaaki Masuda https://orcid.org/0000-0002-6341-2438
Kensuke Koike https://orcid.org/0000-0003-4428-2348
Takeo Toshima https://orcid.org/0000-0003-4019-8288
Hidetoshi Eguchi https://orcid.org/0000-0002-2318-1129
Koshi Mimori https://orcid.org/0000-0003-3897-9974

REFERENCES

1. Cheng Y, He C, Wang M, et al. Targeting epigenetic regulators for cancer therapy: mechanisms and advances in clinical trials. *Signal Transduct Target Ther*. 2019;4:62.
2. Dawson MA, Kouzarides T, Huntly BJ. Targeting epigenetic readers in cancer. *N Engl J Med*. 2012;367(7):647-657.
3. Lovén J, Hoke HA, Lin CY, et al. Selective inhibition of tumor oncogenes by disruption of super-enhancers. *Cell*. 2013;153(2):320-334.
4. Rahman S, Sowa ME, Ottinger M, et al. The Brd4 extraterminal domain confers transcription activation independent of pTEFb by recruiting multiple proteins, including NSD3. *Mol Cell Biol*. 2011;31(13):2641-2652.
5. Sinha A, Faller DV, Denis GV. Bromodomain analysis of Brd2-dependent transcriptional activation of cyclin a. *Biochem J*. 2005;387(Pt 1):257-269.
6. Sun HY, Du ST, Li YY, Deng GT, Zeng FR. Bromodomain and extra-terminal inhibitors emerge as potential therapeutic avenues for gastrointestinal cancers. *World J Gastrointest Oncol*. 2022;14(1):75-89.
7. Dhalluin C, Carlson JE, Zeng L, He C, Aggarwal AK, Zhou MM. Structure and ligand of a histone acetyltransferase bromodomain. *Nature*. 1999;399(6735):491-496.
8. Gilan O, Rioja I, Knezevic K, et al. Selective targeting of BD1 and BD2 of the BET proteins in cancer and immunoinflammation. *Science*. 2020;368(6489):387-394.
9. Fu LL, Tian M, Li X, et al. Inhibition of BET bromodomains as a therapeutic strategy for cancer drug discovery. *Oncotarget*. 2015;6(8):5501-5516.
10. Sahai V, Redig AJ, Collier KA, Eckerdt FD, Munshi HG. Targeting BET bromodomain proteins in solid tumors. *Oncotarget*. 2016;7(33):53997-54009.
11. Hu Y, Zhou J, Ye F, et al. BRD4 inhibitor inhibits colorectal cancer growth and metastasis. *Int J Mol Sci*. 2015;16(1):1928-1948.
12. Stathis A, Bertoni F. BET proteins as targets for anticancer treatment. *Cancer Discov*. 2018;8(1):24-36.
13. Donati B, Lorenzini E, Ciarrocchi A. BRD4 and cancer: going beyond transcriptional regulation. *Mol Cancer*. 2018;17(1):164.
14. Pérez-Salvia M, Esteller M. Bromodomain inhibitors and cancer therapy: from structures to applications. *Epigenetics*. 2017;12(5):323-339.
15. Ba M, Long H, Yan Z, et al. BRD4 promotes gastric cancer progression through the transcriptional and epigenetic regulation of c-MYC. *J Cell Biochem*. 2018;119(1):973-982.
16. Lee JW, Park TG, Bae SC. Involvement of RUNX and BRD family members in restriction point. *Mol Cells*. 2019;42(12):836-839.
17. Zhu Z, Song J, Guo Y, et al. LAMB3 promotes tumour progression through the AKT-FOXO3/4 axis and is transcriptionally regulated by the BRD2/acetylated ELK4 complex in colorectal cancer. *Oncogene*. 2020;39(24):4666-4680.
18. Lambert JP, Picaud S, Fujisawa T, et al. Interactome rewiring following pharmacological targeting of BET bromodomains. *Mol Cell*. 2019;73(3):621-638.
19. Tögel L, Nightingale R, Chueh AC, et al. Dual targeting of bromodomain and extraterminal domain proteins, and WNT or MAPK signaling, inhibits c-MYC expression and proliferation of colorectal cancer cells. *Mol Cancer Ther*. 2016;15(6):1217-1226.
20. Hashiguchi Y, Muro K, Saito Y, et al. Japanese Society for Cancer of the colon and Rectum. Japanese Society for Cancer of the colon and Rectum (JSCCR) guidelines 2019 for the treatment of colorectal cancer. *Int J Clin Oncol*. 2020;25(1):1-42.
21. Kouyama Y, Masuda T, Fujii A, et al. Oncogenic splicing abnormalities induced by DEAD-box helicase 56 amplification in colorectal cancer. *Cancer Sci*. 2019;110(10):3132-3144.
22. Benjamini Y, Hochberg Y. Controlling the false discovery rate: a practical and powerful approach to multiple testing. *J R Stat Soc B Methodol*. 1995;57(1):289-300.
23. Sato K, Masuda T, Hu Q, et al. Phosphoserine phosphatase is a novel prognostic biomarker on chromosome 7 in colorectal cancer. *Anticancer Res*. 2017;37(5):2365-2371.
24. Ueda M, Iguchi T, Nambara S, et al. Overexpression of transcription termination factor 1 is associated with a poor prognosis in patients with colorectal cancer. *Ann Surg Oncol*. 2015;22(Suppl 3):S1490-S1498.
25. Kobayashi Y, Masuda T, Fujii A, et al. Mitotic checkpoint regulator RAE1 promotes tumor growth in colorectal cancer. *Cancer Sci*. 2021;112(8):3173-3189.
26. Masuda T, Xu X, Dimitriadis EK, Lahusen T, Deng CX. "DNA binding region" of BRCA1 affects genetic stability through modulating the intra-S-phase checkpoint. *Int J Biol Sci*. 2016;12(2):133-143.
27. Sato K, Masuda T, Hu Q, et al. Novel oncogene 5MP1 reprograms c-Myc translation initiation to drive malignant phenotypes in colorectal cancer. *EBioMedicine*. 2019;44:387-402.
28. Koike K, Masuda T, Sato K, et al. GET4 is a novel driver gene in colorectal cancer that regulates the localization of BAG6, a nucleo-cytoplasmic shuttling protein. *Cancer Sci*. 2022;113(1):156-169.
29. Tan Y, Wang L, Du Y, et al. Inhibition of BRD4 suppresses tumor growth in prostate cancer via the enhancement of FOXO1 expression. *Int J Oncol*. 2018;53(6):2503-2517.

30. Dong X, Hu X, Chen J, Hu D, Chen LF. BRD4 regulates cellular senescence in gastric cancer cells via E2F/miR-106b/p21 axis. *Cell Death Dis*. 2018;9(2):203.

31. Karimian A, Ahmadi Y, Yousefi B. Multiple functions of p21 in cell cycle, apoptosis and transcriptional regulation after DNA damage. *DNA Repair (Amst)*. 2016;42:63-71.

32. Zheng X, Song J, Yu C, et al. Single-cell transcriptomic profiling unravels the adenoma-initiation role of protein tyrosine kinases during colorectal tumorigenesis. *Signal Transduct Target Ther*. 2022;7(1):60.

33. Wu Y, Yang S, Ma J, et al. Spatiotemporal immune landscape of colorectal cancer liver metastasis at single-cell level. *Cancer Discov*. 2022;12(1):134-153.

34. Zhang P, Dong Z, Cai J, et al. BRD4 promotes tumor growth and epithelial-mesenchymal transition in hepatocellular carcinoma. *Int J Immunopathol Pharmacol*. 2015;28(1):36-44.

35. Alqahtani A, Choucair K, Ashraf M, et al. Bromodomain and extra-terminal motif inhibitors: a review of preclinical and clinical advances in cancer therapy. *Future Sci OA*. 2019;5(3):FSO372.

36. Zuber J, Shi J, Wang E, et al. RNAi screen identifies Brd4 as a therapeutic target in acute myeloid leukaemia. *Nature*. 2011;478(7370):524-528.

37. Bandopadhayay P, Bergthold G, Nguyen B, et al. BET bromodomain inhibition of MYC-amplified medulloblastoma. *Clin Cancer Res*. 2014;20(4):912-925.

38. Shu S, Lin CY, He HH, et al. Response and resistance to BET bromodomain inhibitors in triple-negative breast cancer. *Nature*. 2016;529(7586):413-417.

39. Klingbeil O, Lesche R, Gelato KA, Haendler B, Lejeune P. Inhibition of BET bromodomain-dependent XIAP and FLIP expression sensitizes KRAS-mutated NSCLC to pro-apoptotic agents. *Cell Death Dis*. 2016;7(9):e2365.

40. Calder J, Nagelberg A, Luu J, Lu D, Lockwood WW. Resistance to BET inhibitors in lung adenocarcinoma is mediated by casein kinase phosphorylation of BRD4. *Oncogenesis*. 2021;10(3):27.

41. Fong CY, Gilan O, Lam EY, et al. BET inhibitor resistance emerges from leukaemia stem cells. *Nature*. 2015;525(7570):538-542.

42. Rathert P, Roth M, Neumann T, et al. Transcriptional plasticity promotes primary and acquired resistance to BET inhibition. *Nature*. 2015;525(7570):543-547.

43. Shorstova T, Foulkes WD, Witcher M. Achieving clinical success with BET inhibitors as anti-cancer agents. *Br J Cancer*. 2021;124(9):1478-1490.

44. Qin AC, Jin H, Song Y, et al. The therapeutic effect of the BRD4-degrading PROTAC A1874 in human colon cancer cells. *Cell Death Dis*. 2020;11(9):805.

45. Sun XF. p73 overexpression is a prognostic factor in patients with colorectal adenocarcinoma. *Clin Cancer Res*. 2002;8(1):165-170.

46. Romagosa C, Simonetti S, López-Vicente L, et al. p16(Ink4a) overexpression in cancer: a tumor suppressor gene associated with senescence and high-grade tumors. *Oncogene*. 2011;30(18):2087-2097.

47. Jost CA, Marin MC, Kaelin WG Jr. p73 is a simian [correction of human] p53-related protein that can induce apoptosis. *Nature*. 1997;389(6647):191-194.

SUPPORTING INFORMATION

Additional supporting information can be found online in the Supporting Information section at the end of this article.